

Supplemental Material - Wavefield distortion imaging of Earth's deep mantle

Sebastian Rost, Daniel A. Frost, Andy Nowacki, Laura Cobden

1. Introduction

This document contains the supplemental figures for the manuscript *Wavefield distortion imaging of Earth's deep mantle*. Fig. 1 shows the location of detected multipathing in the dataset. Fig. 2 shows the additional *S*-wave dataset from the northern Canadian POLARIS stations as described in the main text. The dataset is sparser than the *P*-wave dataset, but shows similar structures. Due to the sparsity of the dataset a more detailed analysis of this dataset is difficult. Fig. 3 shows the measured traveltimes residuals relative to 1D Earth models IASP91 (Kennett and Engdahl, 1991) for the Pacific. The strongest traveltime deviations are visible where we detect the edges of the anomalous velocity structures. Fig. 4 shows the radial and transverse slowness deviations relative to the great circle path and IASP91 (Kennett and Engdahl, 1991) arrival angles.

2. Supplemental Figures

3. References

Kennett, B., Engdahl, E., 1991. Traveltimes for global earthquake location and phase identification. *Geophysical Journal International* 105 (2), 429–465.

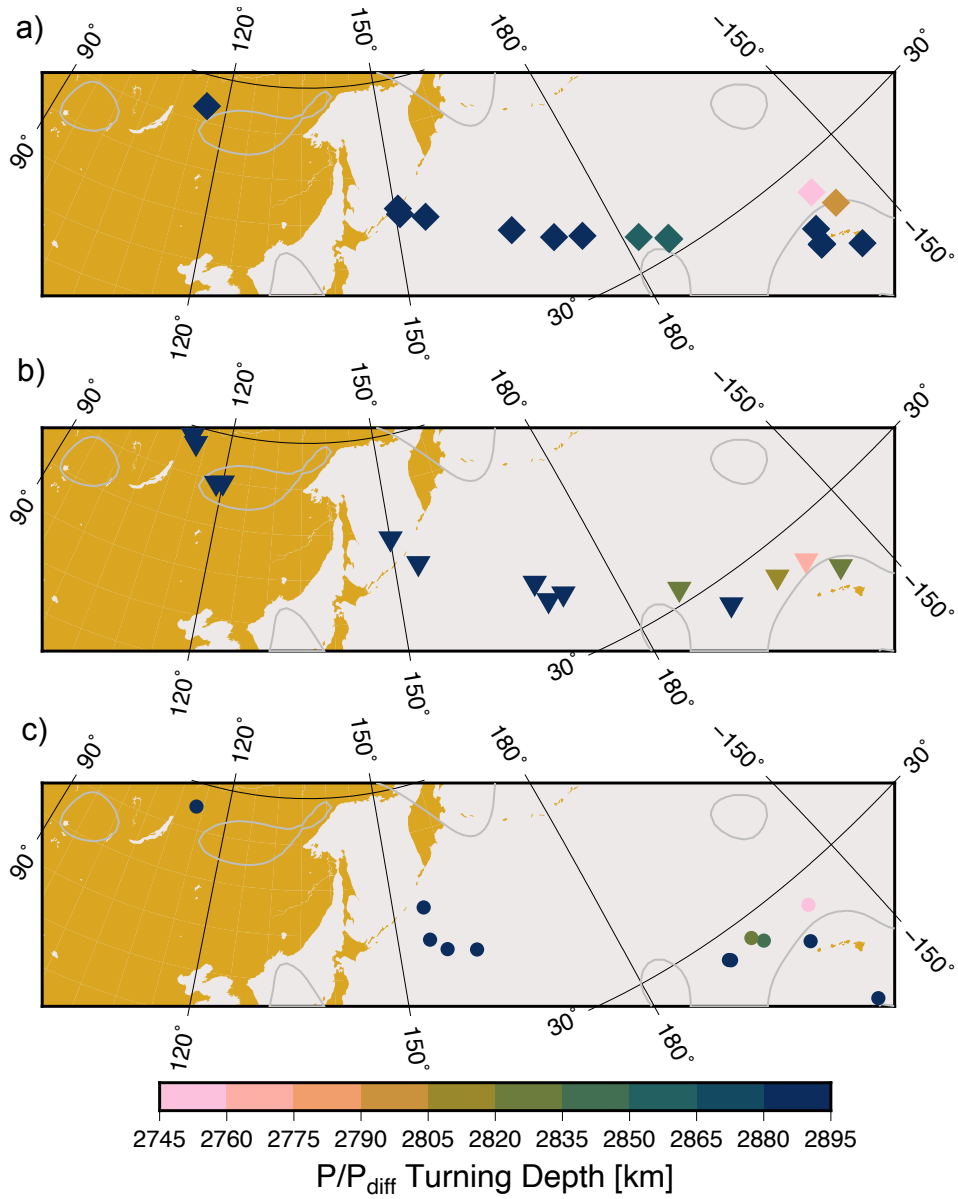


Figure 1: Location of multipathed events detected in the P -wave dataset. a) P/P_{diff} turning point location of backazimuth multipathed events, which are defined as multipathed events where the two arrivals show similar slowness but strongly different backazimuths. b) as a) but for slowness multipathed events, which are defined as events where the two arrivals show similar backazimuths but strongly different slownesses. c) as a) but for slowness-backazimuth multipathed events, which show both slowness and backazimuth deviations of the multiple detected arrivals.

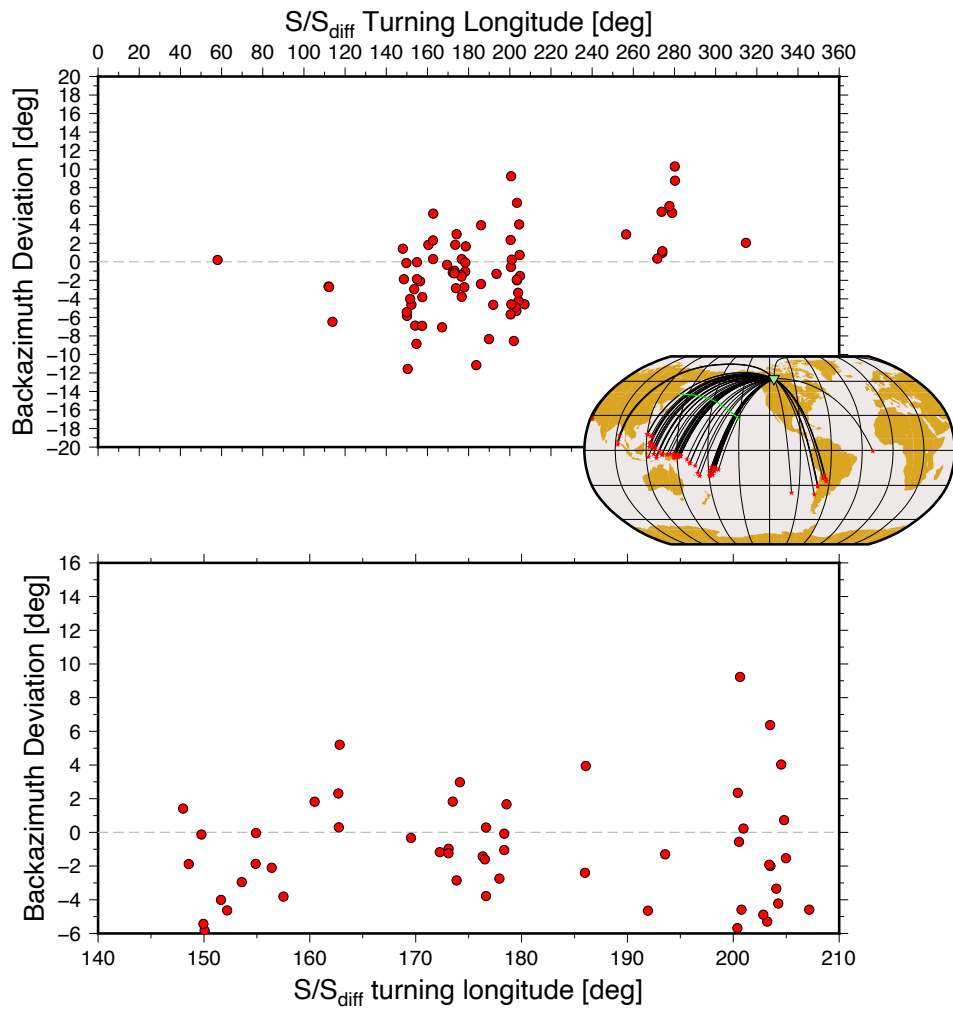


Figure 2: Measured S/S_{diff} backazimuth deviation displayed at turning point longitude. Insert shows the event locations and great circle paths of the S -wave dataset. Lower panel shows the events sampling the Pacific along the profile shown in green in the insert.

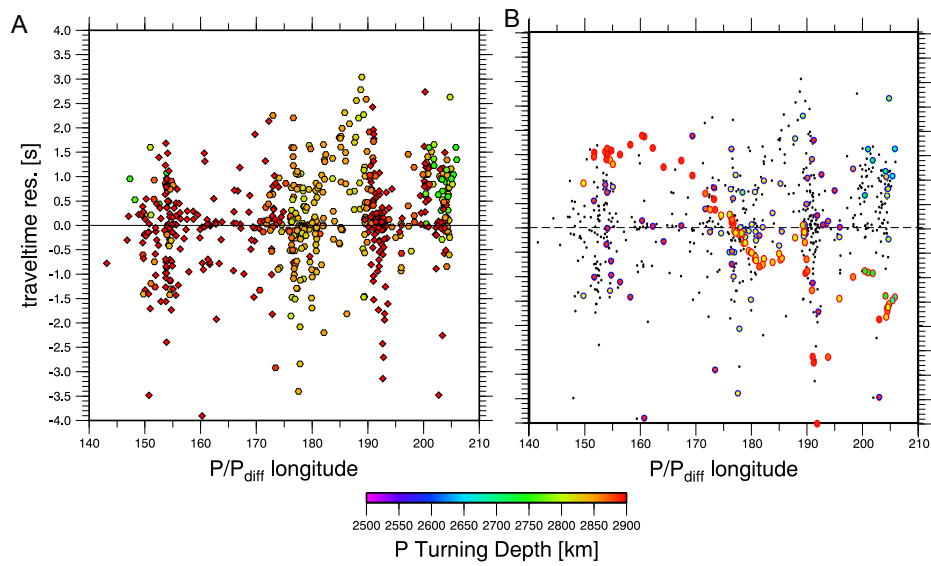


Figure 3: A) Measured P/P_{diff} traveltime residuals relative to IASP91 (Kennett and Engdahl, 1991) shown at turning point longitude for P and at the halfway point of the P_{diff} path. Color indicates turning point depth. B) Traveltime residuals relative to IASP91 (Kennett and Engdahl, 1991) through best-fitting Pacific model (red symbols outline). Measured travetime residuals from dataset as small symbols with the sparse dataset used to fit the data shown as large symbols with blue outline.

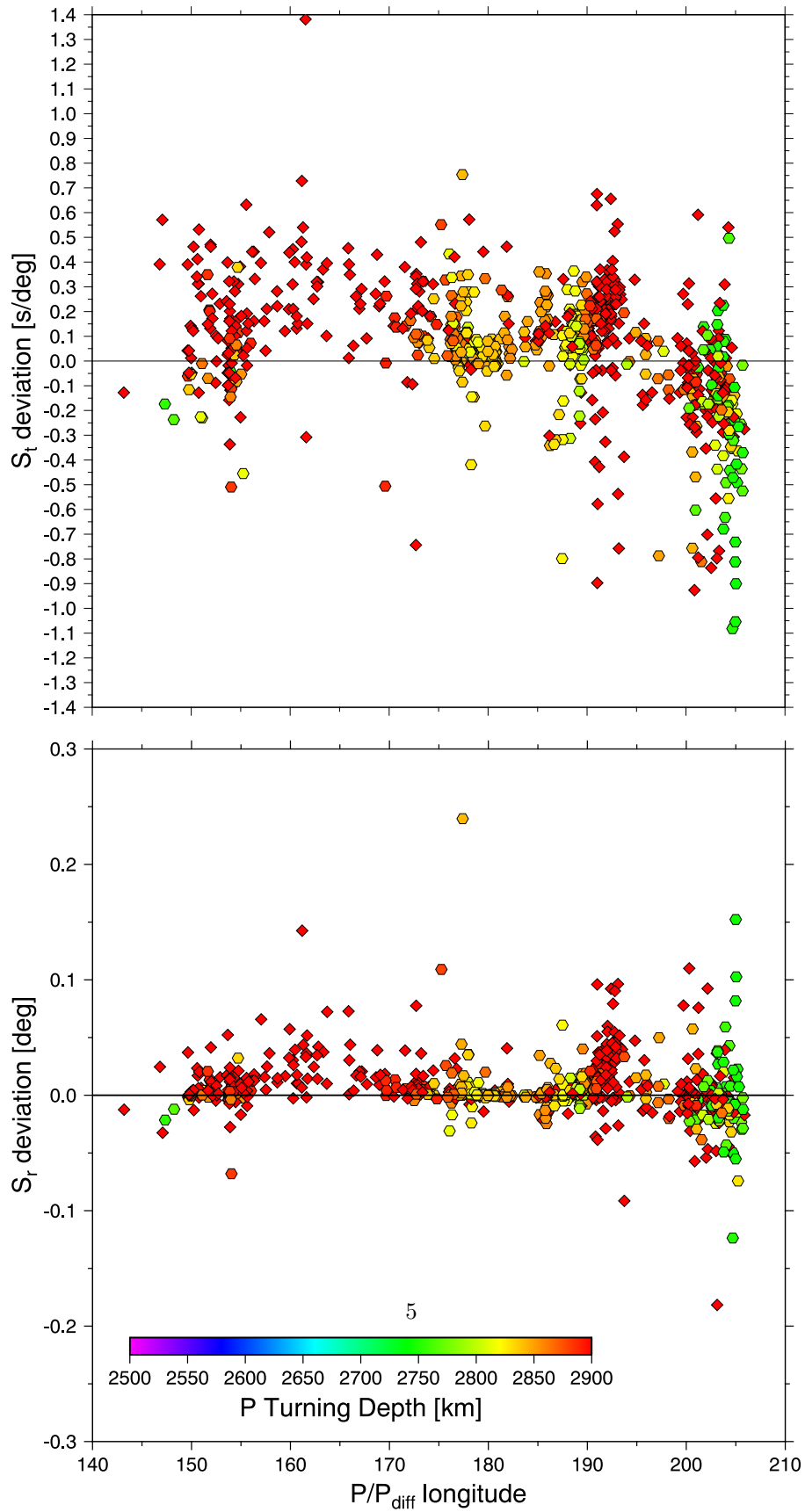


Figure 4: Measured slowness vector deviations shown as radial and transverse slowness residuals relative to the IASP91 (Kennett and Engdahl, 1991) slowness for the respective source-receiver combination.